ON HYDRODYNAMIC STABILITY OF DEAN FLOW BY USING ENERGY GRADIENT METHODS

H. Nowruzi **H. Ghassemi***

Department of Maritime Engineering
Amirkabir University of Technology (Tehran Polytechnic)
Tehran, Iran

S. S. Nourazar

Department of Mechanical Engineering
Amirkabir University of Technology (Tehran Polytechnic)
Tehran, Iran

ABSTRACT

In the present paper, we investigate the hydrodynamic instability of Dean flow under different Dean numbers ranging from 1 to 2500, curvature ratios from 0.0001 up to 1000 and temperatures ranging from 273.15 K to 373.15 K. To study of fluid flow instability, analytical velocity profiles under intended conditions and energy gradient function K in the energy gradient method are evaluated. The results of present study show that, as the curvature ratio increases the flow becomes more stable. Moreover, no regular and significant effects on the energy gradient function K were achieved by increasing of temperatures. We found that, the origin of instability in the entire flow field is located on the inner wall of the parallel curved walls, especially for larger curvature ratios. We also reported the critical value of the energy gradient function K for the onset of instability corresponding to the critical Dean number.

Keywords: Hydrodynamic stability, Dean flow, Analytical method, Energy gradient method.

1. INTRODUCTION

Dean fluid flow in curved paths is a prevalent phenomenon in macro-scale mechanical systems and micro-nano electromechanical systems (MEMS/NEMS). Dean flow refers to the problem of incompressible viscous fluid flow between two parallel curved walls as shown in Fig. 1 [1]. This appellation is related to study of Dean in 1928 [2]. In Dean flow, centrifugal forces lead to counter-rotating vortex motion mounted on the axial flow which is known as the secondary flow [1]. Under specific critical Dean flow condition, due to imbalance among radial centrifugal forces and pressure gradient, hydrodynamic instability will be occurred in form of additional pairs of counter-rotating vortices. This flow hydrodynamic instability refers to Dean hydrodynamic instability and additional vortices are called Dean vortices. Dean [2] presented the equations of motion and continuity for incompressible viscous fluid flow between two parallel curved walls with small curvature, mathematically. Afterward, he added infinite axially periodic small disturbance to axisymmetry basic flow under regardless of gravitational effects. Then, linearized characteristics equation for the eigenvalue problem according to the growth rate of the disturbance is solved by Dean and he determined the critical condition for onset of flow instability. Dean's flow pioneering study for this problem has been considered as a classical example in field of flow stability analysis. Until now, Dean flow is comprehensively investigated by many

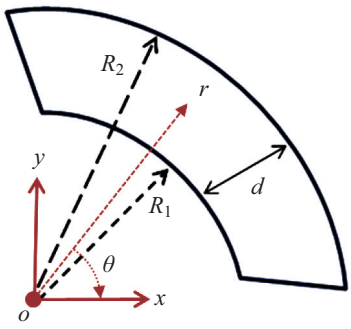


Fig. 1 A schematic of the problem; r is cross-stream direction and θ is stream-wise direction.

* Corresponding author (gasemi@aut.ac.ir)

DOI : 10.1017/jmech.2017.112
Copyright © 2018 The Society of Theoretical and Applied Mechanics
https://doi.org/10.1017/jmech.2017.112 Published online by Cambridge University Press

researchers via experimental, numerical and mathematical models [3-10]. For example, Reid [11] studied the stability of viscous flow in a curved channel by using two method of approximated solution. Reid and Harris [12] investigated the stability of a viscous fluid contained between two rigid walls and heated from below by using exact solution of the sixth-order differential equation. They presented the detailed results on the curve of neutral stability and the cell pattern at the onset of instability. The eigenvalue problem arising from linear hydrodynamic instability of Dean flow is also studied by Bahl [13] and Chandrasekhar's [14] with Fourier expansion technique. However, despite of comprehensive study on Dean hydrodynamic instability [15-24], this problem isn't well-known. Because, cited works dealing with limiting cases of Dean flow when the ratio of the gap width to the radii tends to zero, where radius is infinite or gap width is very small. Moreover, up to now, the local positions in a Dean flow where the instability is originated from there, is not well specified under different Dean numbers, curvature ratios and temperatures.

Recently, Dou [25, 26] proposed the energy gradient method to investigate of fluid flow field instability and determination of local positions with the highest probability of instability occurrence. Therefore, our goal in the present paper is to study the instability (i.e. onset of instability) of Dean flow under comprehensive different Dean numbers, curvature ratios and temperatures by using the energy gradient method. To this accomplishment, different Dean numbers ranging from 1 to 2500, temperatures ranging from 273.15 K to 373.15 K and curvature ratios of very low value of 0.0001 up to very high quantity of 1000 are considered. The results of our investigation show that by increasing of the curvature ratios and decreasing of Dean number, maximum of energy gradient function K is diminished and the flow becomes more stable.

2. PHYSICAL MODEL

Figure 1 shows the schematic of fluids flow between two parallel curved walls which is known as Dean Flow. As may be seen in Fig. 1, z axis coincides by the axis of cylinder and R_1, R_2 are inner and outer radii, respectively.

In cylindrical coordinates (r, θ, z) and velocity components of $U = (u_r, u_\theta, u_z)$, the Navier-Stokes equations for laminar, viscous and incompressible flow are expressed as:

$$\frac{Du_r}{Dt}-\frac{u_\theta^2}{r}=-\frac{1}{\rho}\frac{\partial p}{\partial r}+\upsilon\left(\Delta u_r-\frac{u_r}{r^2}-\frac{2}{r^2}\frac{\partial u_\theta}{\partial\theta}\right), \tag{1}$$

$$\frac{Du_\theta}{Dt}+\frac{u_r u_\theta}{r}=-\frac{1}{\rho}\frac{1}{r}\frac{\partial p}{\partial\theta}+\upsilon\left(\Delta u_\theta-\frac{u_\theta}{r^2}+\frac{2}{r^2}\frac{\partial u_r}{\partial\theta}\right), \tag{2}$$

$$\frac{Du_z}{Dt}=-\frac{1}{\rho}\frac{\partial p}{\partial z}+\upsilon\Delta u_z, \tag{3}$$

where

$$\frac{D}{Dt}=\frac{\partial}{\partial t}+u_r\frac{\partial}{\partial r}+\frac{u_\theta}{r}\frac{\partial}{\partial\theta}+u_z\frac{\partial}{\partial z}, \tag{4}$$

$$\Delta=\frac{\partial^2}{\partial r^2}+\frac{1}{r}\frac{\partial}{\partial r}+\frac{1}{r^2}\frac{\partial^2}{\partial\theta^2}+\frac{\partial^2}{\partial z^2}. \tag{5}$$

and continuity equation is

$$\frac{\partial u_r}{\partial r}+\frac{u_r}{r}+\frac{1}{r}\frac{\partial u_\theta}{\partial\theta}+\frac{\partial u_z}{\partial z}=0 \tag{6}$$

By assuming the unidirectional flow, velocity components in basic flow have form of $u_r = u_z = 0$ and $u_\theta = V(r)$. In this case, the Navier–Stokes equations in radial and circumferential directions for steady flows will be reduced to

$$\frac{1}{\rho}\frac{\partial p}{\partial r}=\frac{V^2}{r}, \tag{7}$$

$$\frac{2M}{r}=DD_*\,\mathrm{V}-\frac{\mathrm{V}}{r^2}. \tag{8}$$

with no-slip boundary conditions as follows:

$$V(r)=0 \quad @ \quad r=R_1;R_2 \tag{9}$$

where,

$$\begin{cases} D=\dfrac{d}{dr} \\ D_*=\dfrac{d}{dr}+\dfrac{1}{r} \\ M=\dfrac{1}{2\rho\upsilon}\left(\dfrac{\partial p}{\partial\theta}\right)_0 \end{cases} \tag{10}$$

here, ρ, υ and $\left(\frac{\partial p}{\partial\theta}\right)_0$ are density, kinematic viscosity and constant azimuthal pressure gradient, respectively. Integrating Eq. (8) and using the boundary conditions Eq. (9) give the solution of velocity distribution as,

$$V(r)=Ar+\frac{B}{r}+Mr\ln r \tag{11}$$

where, the constant of A and B are given by:

$$\begin{cases} A=\dfrac{M\left(\ln R_2-\left(\dfrac{R_1}{R_2}\right)^2\ln R_1\right)}{\left(\dfrac{R_1}{R_2}\right)^2-1} \\ B=\dfrac{M\left(R_1^2\ln\dfrac{R_1}{R_2}\right)}{\left(\dfrac{R_1}{R_2}\right)^2-1} \end{cases} \tag{12}$$

Dean number (Dn) may be defined as [12 or 27]:

$$Dn=\mathrm{Re}\left(d/R_1\right)^{0.5} \tag{13}$$

here, $\delta = d/R_1$ is the curvature ratio, $d = R_2 - R_1$ is gap

https://doi.org/10.1017/jmech.2017.112 Published online by Cambridge University Press

width and Re is Reynolds number as follows:

$$\mathrm{Re}=\frac{V_m d}{\upsilon} \tag{14}$$

where, V_m as an average velocity is:

$$V_m=\frac{1}{R_2-R_1}\int_{R_1}^{R_2}V(r)dr$$

$$=\frac{MR_2}{4\left(1-\frac{R_1}{R_2}\right)}\left[\frac{\left(\left(\frac{R_1}{R_2}\right)^2-1\right)^2-\left(2\frac{R_1}{R_2}\ln\frac{R_1}{R_2}\right)^2}{\left(\frac{R_1}{R_2}\right)^2-1}\right] \tag{15}$$

3. ENERGY GRADIENT METHOD

To investigate of flow instability and transition from laminar to turbulence, energy gradient method is proposed by Dou [25] in 2004. The basic definitions and the detail of fundamental concepts of the energy gradient method may be found in Refs. [26, 28-31]. For the convenience of the readers and without loss of the generality, the basic concepts of energy gradient method is described in the following.

According to energy gradient method, flow field is considered as an energy field. Energy gradient method is expressing that, the gradient of total mechanical energy in the cross-stream direction (i.e. transverse direction) of the main flow and the total mechanical energy loss from viscous friction in the stream-wise direction governs fluid flow instability for a given disturbance. It is proposed that the velocity disturbance will be amplified by energy gradient in cross-stream direction, whereas this disturbance will be decayed by viscous friction loss in the stream-wise direction. Indeed, the relative magnitude of energy gradient amplification in the cross-stream direction compared to viscous friction damping in the stream-wise direction is a stability criterion as follows [28, 29]:

$$F=\frac{\Delta E}{\Delta H}=\frac{\left(\frac{\partial E}{\partial n}\frac{2\bar{A}}{\pi}\right)}{\left(\frac{\partial H}{\partial s}\frac{\pi}{\omega}V\right)}=\frac{2}{\pi^2}K\frac{\bar{A}\omega}{V}=\frac{2}{\pi^2}K\frac{v_m'}{V}<Const. \tag{16}$$

where

$$K=\frac{\partial E/\partial n}{\partial H/\partial s} \tag{17}$$

here, ΔE and ΔH are the gradient of total mechanical energy of unit volumetric fluid in the cross-stream direction and the loss of total mechanical energy of unit volumetric fluid in the stream-wise direction, respectively. $E=p+\frac{1}{2}\rho V^2$ is total mechanical energy (where, p is fluid pressure) and H is the energy loss per unit volumetric fluid. Further, n, s, $\bar{A}$, ω and v_m' are along the cross-stream direction, along the stream-wise direction, amplitude of the disturbance distance, frequency of the disturbance and amplitude of the disturbance of velocity $v'=v_m'\cos(\omega t+\varphi_0)$, respectively. In addition, K as dimensionless field variable that represents the ratio of the cross-stream energy gradient and the rate of the energy loss along the stream-wise direction. According to Eq. (16), one can be concluded that, the fluid flow become unstable with increasing of the value of F and we may find a constant value of F that flow will be stable below this value. On the other hands, the instability of fluid flow is depended on the value of K and the amplitude of the relative disturbance velocity ($\frac{v_m'}{V}$). For given disturbance velocity, the maximum of K ($K_{\max}$) as stability parameter determines the flow stability. So that, if $K_{\max}<K_c$, the flow is stable and in case of $K_{\max}>K_c$, flow will be unstable, where, K_c is representative of the critical value of $K_{\max}$.

3.1 Energy Gradient Method Applied to Dean Flow

The gradient of the total mechanical energy in the cross-stream (i.e. as may be seen in Fig. 1, $n\approx r$) direction is:

$$\frac{\partial E}{\partial r}=\frac{\partial\left(p+\rho V^2/2\right)}{\partial r}=\frac{\partial p}{\partial r}+\rho V\frac{\partial V}{\partial r} \tag{18}$$

According to Eq. (7), we can redefine the Eq. (18) as follows:

$$\frac{\partial E}{\partial r}=\frac{\partial\left(p+\rho V^2/2\right)}{\partial r}=\rho\frac{V^2}{r}+\rho V\frac{\partial V}{\partial r}=\rho\left[V\frac{\partial V}{\partial r}+\frac{V^2}{r}\right] \tag{19}$$

By substituting the Eq. (11) into Eq. (19), the energy gradient in the cross-stream direction is expressed as follows:

$$\frac{\partial E}{\partial r}=$$

$$\rho\left[\left(Ar+\frac{B}{r}+Mr\ln r\right)\left(A-\frac{B}{r^2}+M\left(\ln r+1\right)\right)+\frac{\left(Ar+\frac{B}{r}+Mr\ln r\right)^2}{r}\right] \tag{20}$$

For pressure driven flow to calculate of energy loss along the stream-wise direction in the curved path, we have [29]:

$$\frac{\partial H}{\partial s}=\frac{2\tau}{r}+\frac{\partial\tau}{\partial r} \tag{21}$$

where, τ is a shear stress and according to the velocity gradient obtained from Eq. (11), the shear stress has the

https://doi.org/10.1017/jmech.2017.112 Published online by Cambridge University Press

following form:

$$\tau = \mu\left(\frac{\partial V}{\partial r} - \frac{V}{r}\right) \tag{22}$$

here, μ is the dynamic viscosity. Thus, energy loss may be redefined as:

$$\frac{\partial H}{\partial s} = 2\frac{\mu}{r}\left(\frac{\partial V}{\partial r} - \frac{V}{r}\right) + \mu\left(\frac{\partial^2 V}{\partial r^2} + \frac{V}{r^2} - \frac{1}{r}\frac{\partial V}{\partial r}\right) = \frac{\mu}{r}\frac{\partial V}{\partial r} - \frac{\mu V}{r^2} + \mu\frac{\partial^2 V}{\partial r^2} \tag{23}$$

By substituting the Eq. (11) into Eq. (23), the energy loss in the stream-wise direction is expressed as follows:

$$\frac{\partial H}{\partial s} = \mu\left[\frac{1}{r}\left(A - \frac{B}{r^2} + M\left(\ln r + 1\right)\right) - \frac{\left(Ar + \frac{B}{r} + Mr\ln r\right)}{r^2} + \left(\frac{2B}{r^3} + \frac{M}{r}\right)\right] \tag{24}$$

Now, by substituting the Eqs. (20) and (23) into Eq. (17), the energy gradient function K (i.e. stability parameter) is defined by:

$$K = \frac{\partial E/\partial r}{\partial H/\partial s} = \frac{\rho\left[\left(Ar + \frac{B}{r} + Mr\ln r\right)\left(A - \frac{B}{r^2} + M\left(\ln r + 1\right)\right) + \frac{\left(Ar + \frac{B}{r} + Mr\ln r\right)^2}{r}\right]}{\mu\left[\frac{1}{r}\left(A - \frac{B}{r^2} + M\left(\ln r + 1\right)\right) - \frac{\left(Ar + \frac{B}{r} + Mr\ln r\right)}{r^2} + \left(\frac{2B}{r^3} + \frac{M}{r}\right)\right]}$$

$$= \frac{\rho\left[\frac{\left(2A + M + 2M\ln r\right)\left(B + r^2\left(A + M\ln r\right)\right)}{r}\right]}{\mu\left(\frac{2M}{r}\right)}$$

$$= \frac{1}{\upsilon}\left[\frac{B}{2} + B\ln r + \frac{AB}{M} + \frac{Ar^2}{2} + 2Ar^2\ln r + \frac{A^2r^2}{M} + \frac{1}{2}Mr^2\ln r + Mr^2\left(\ln r\right)^2\right] \tag{25}$$

Introducing Eq. (12) into Eq. (25), and by simplifying and rearranging, the final form of the dimensionless parameter of energy gradient function (K) for Dean flow is found as follows:

$$K = \frac{\partial E/\partial r}{\partial H/\partial s} = \frac{\rho}{\mu}\frac{\left[\left(2A + M + 2M\ln r\right)\left(B + r^2\left(A + M\ln r\right)\right)\right]}{2M}$$

$$= \mu\left(\frac{\left(\frac{\partial p}{\partial\theta}\right)_0\left(\left(\frac{R_1}{R_2}\right)^2 - 1\right)\left(1 + 2\ln r\right)}{2\mu} + \frac{\left(\frac{\partial p}{\partial\theta}\right)_0}{\mu}\left[\ln R_2 - \left(\frac{R_1}{R_2}\right)^2\ln R_1\right]\right)\bullet$$

$$\frac{\left(\frac{\left(\frac{\partial p}{\partial\theta}\right)_0}{2\mu}\left[R_1^2\ln\frac{R_1}{R_2}\right] + r^2\left(\frac{\left(\frac{\partial p}{\partial\theta}\right)_0\left(\left(\frac{R_1}{R_2}\right)^2 - 1\right)\ln r}{2\mu} + \frac{\left(\frac{\partial p}{\partial\theta}\right)_0}{2\mu}\left[\ln R_2 - \left(\frac{R_1}{R_2}\right)^2\ln R_1\right]\right)\right)}{\upsilon\left(\frac{\partial p}{\partial\theta}\right)_0\left(\left(\frac{R_1}{R_2}\right)^2 - 1\right)^2} \tag{26}$$

https://doi.org/10.1017/jmech.2017.112 Published online by Cambridge University Press

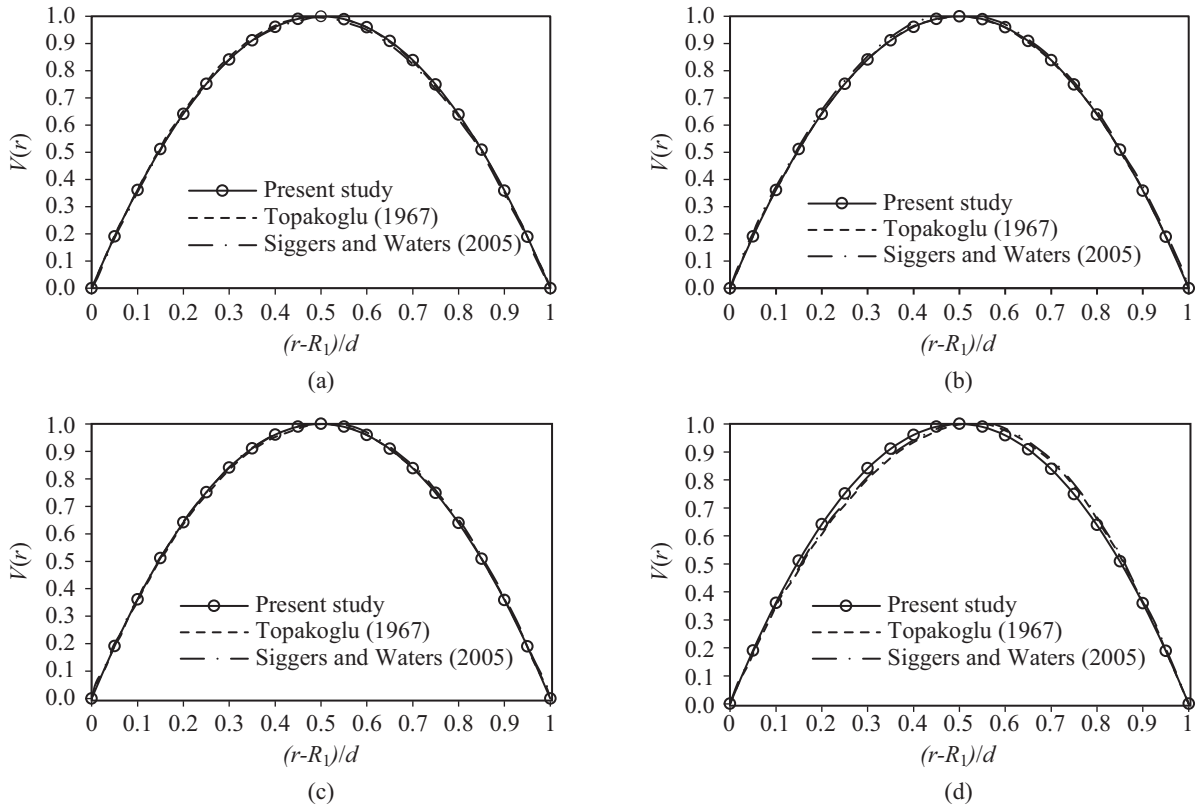


Fig. 2 Normalized axial velocity profiles calculated from the analytical solutions (present study) compared to Topakoglu [32] and Siggers and Waters [33] results for (a) Dn = 1, (b) Dn = 10, (c) Dn = 25 and (d) Dn = 50 under $\delta = 0.01$.

Continued, the results of velocity profile and energy gradient function K for Dean flow under different Dean numbers, temperatures and curvature ratios are presented.

4. RESULTS AND DISCUSSION

In this section, we preliminary compare the obtained analytical normalized velocity profile of the present study with Topakoglu [32] and Siggers and Waters [33] results. These existing normalized velocity profile in Refs. [32, 33] which is obtained by using a series expansion method are valid for Dn < 96. Therefore, our result compared with existing numerical normalized velocity profile [32, 33] for Dn = 1, 10, 25 and 50 under $\delta = 0.01$ and 0.16 in Figs. 2 and 3, respectively. As may be seen in Figs. 2 and 3, an acceptable accordance with the maximum error below the 2.12% is achieved between our results compared to archival data [32, 33]. In addition, it is observed that in the narrow gap condition (i.e. very small curvatures $\delta << 1$), velocity profiles have the form of the parabolic plane Poiseuille flow.

Continued, the results of the effects of different Dean numbers, curvature ratios and temperatures on analytical velocity profile and energy gradient function K as a hydrodynamic stability criteria, are presented.

4.1 Effects of Dean Number

Figures 4, 5 and 6 show the velocity profile for different Dean number (Dn) ranging from 1 to 2500 under the small curvature ratio $\delta = 0.1$ at T = 293.15 K, T = 298.15 K and T = 303.15 K, respectively. As may be seen in Figs. 4, 5 and 6, by increase of Dean flow, the peak of velocity profile is increased. In addition, same trend in analytical velocity profile is evident under different Dean numbers, for all three considered temperatures. The reason for forming the parabolic velocity profile under different Dean number is related to considered small curvature of our geometry (e.g. $\delta = 0.1$ in case of $R_1 = 1$ and $R_2 = 1.1$). Indeed, under the condition of small curvature, the Eqs. (11-15) for velocity profiles lead to the parabolic plane Poiseuille flow. Moreover, comparing between Figs. 3, 4 and 5 show that the different temperatures have an insignificant effect on the peak of the velocity profile under different Dean numbers.

It's notable that, in the present study, the temperature effects are introduced to our current analyses by considering the temperature impression via the variation of water properties such as its viscosity. Indeed, according to Eqs. (11) and (26), thermophysical properties of considered fluid (i.e. water in the present study) are impressive on velocity profile and energy gradient function K. As a result, change of the thermophysical properties of liquid water by varying the temperatures lead to change the velocity profile and the energy gradient function K. More details are presented in subsection 4.2.

https://doi.org/10.1017/jmech.2017.112 Published online by Cambridge University Press

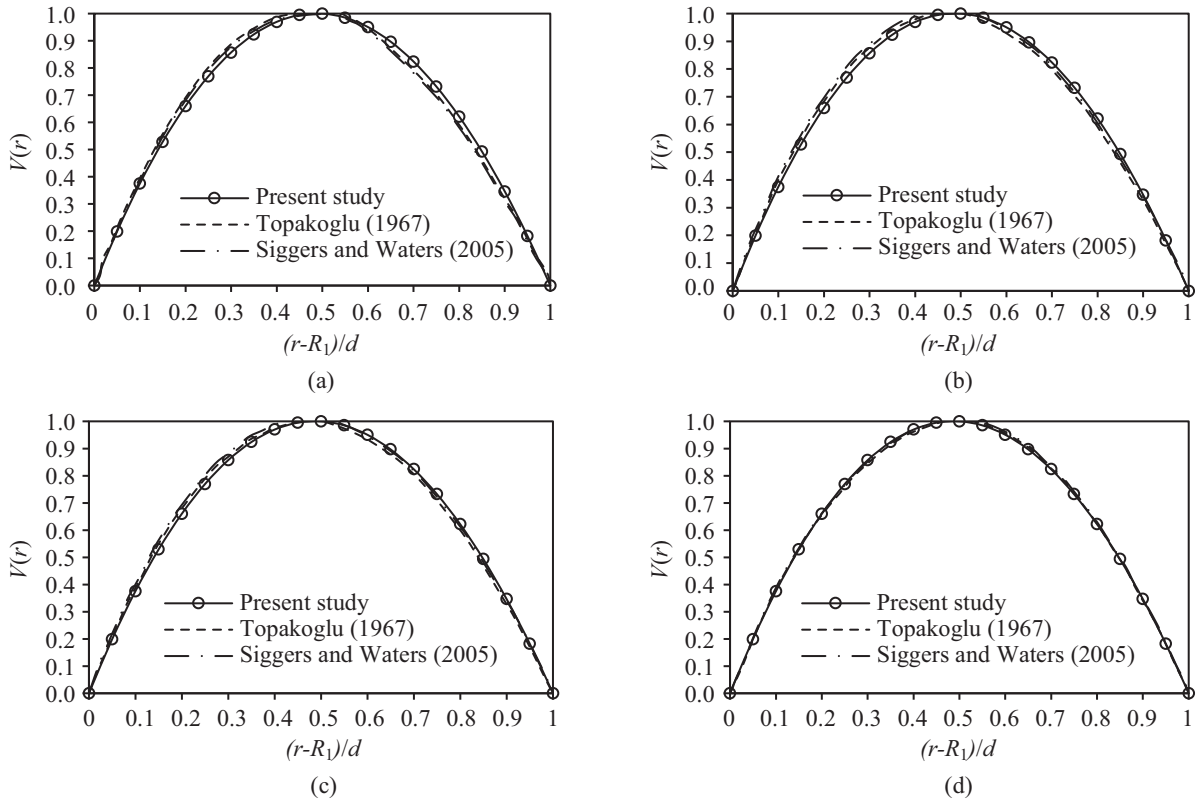


Fig. 3 Normalized axial velocity profiles calculated from the analytical solutions (present study) compared to Topakoglu [32] and Siggers and Waters [33] results for (a) Dn = 1, (b) Dn = 10, (c) Dn = 25 and (d) Dn = 50 under $\delta = 0.16$.

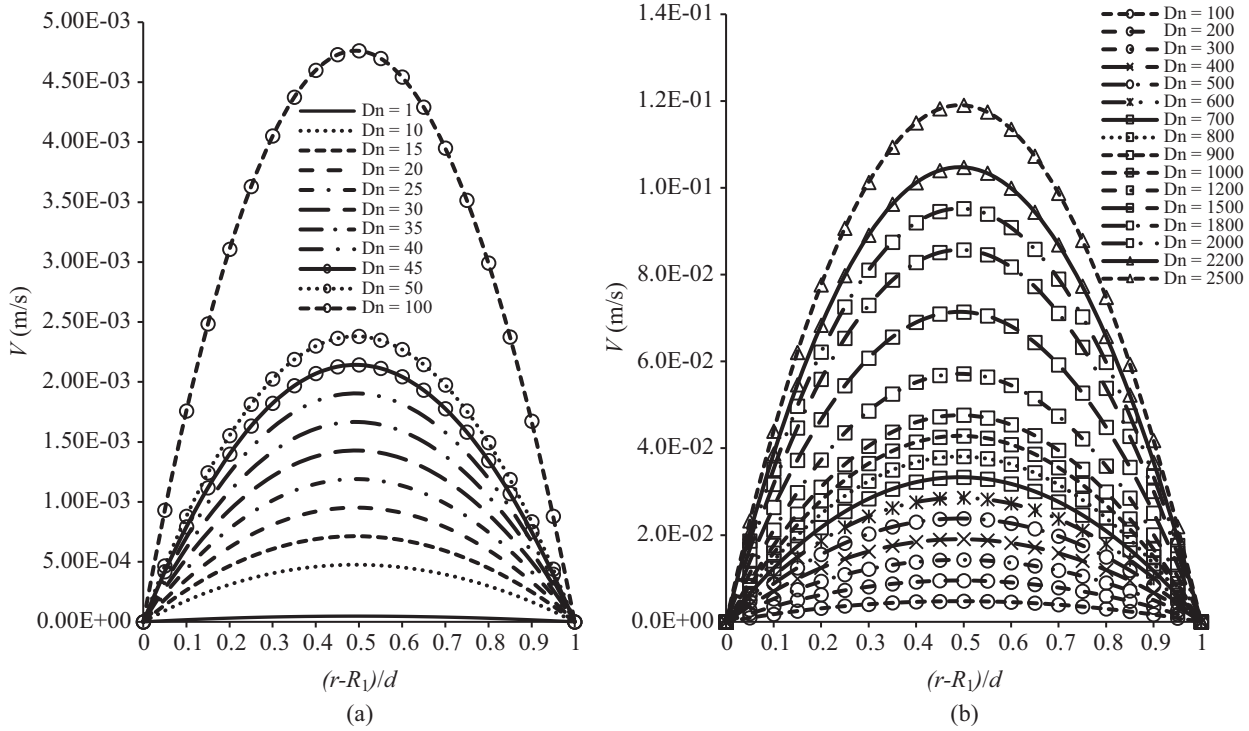


Fig. 4 Velocity profile at different Dean numbers under $\delta = 0.1$ and T = 293.15 K; (a) Dn = 1 to Dn = 100; (b) Dn = 100 to 2500.

https://doi.org/10.1017/jmech.2017.112 Published online by Cambridge University Press

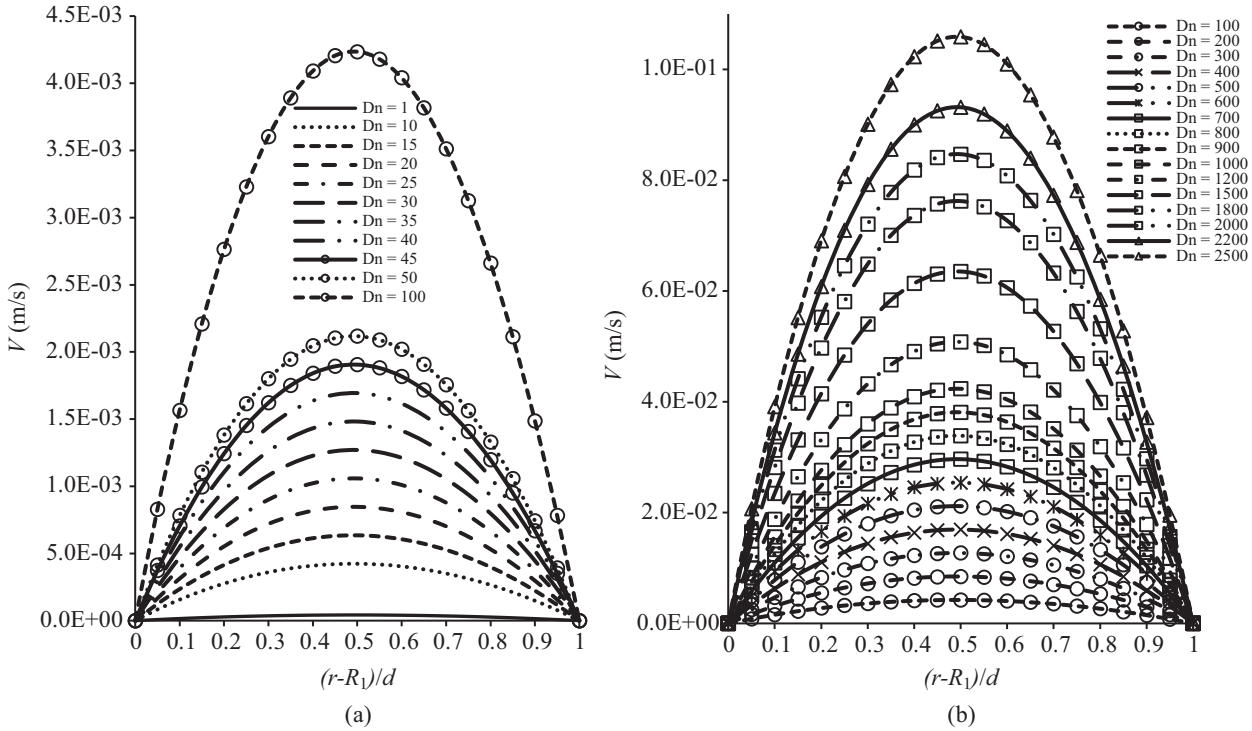


Fig. 5 Velocity profile at different Dean numbers under δ = 0.1 and T = 298.15 K; (a) Dn = 1 to Dn = 100; (b) Dn = 100 to 2500.

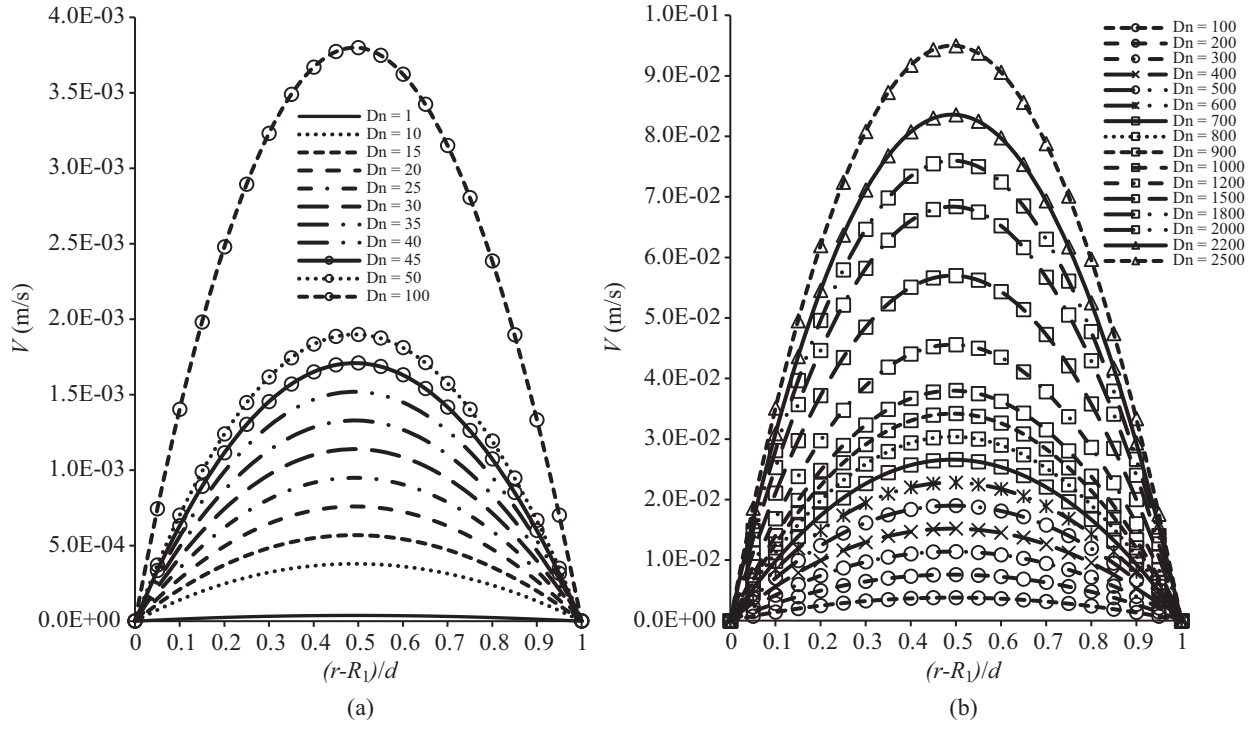


Fig. 6 Velocity profile at different Dean numbers under δ = 0.1 and T = 303.15 K; (a) Dn = 1 to Dn = 100; (b) Dn = 100 to 2500.

For investigation of the effects of Dean number on the Dean flow instability, we present the distribution of absolute value of the dimensionless parameter of energy gradient function K for Dean numbers ranging from 1 to 2500 under small curvature δ = 0.1 at T = 293.15 K, T = 298.15 K and T =303.15 K in Figs. 7, 8 and 9, respectively. As may be seen in Figs. 7, 8 and 9, by increase of Dean numbers, the value of K is increased, for

https://doi.org/10.1017/jmech.2017.112 Published online by Cambridge University Press

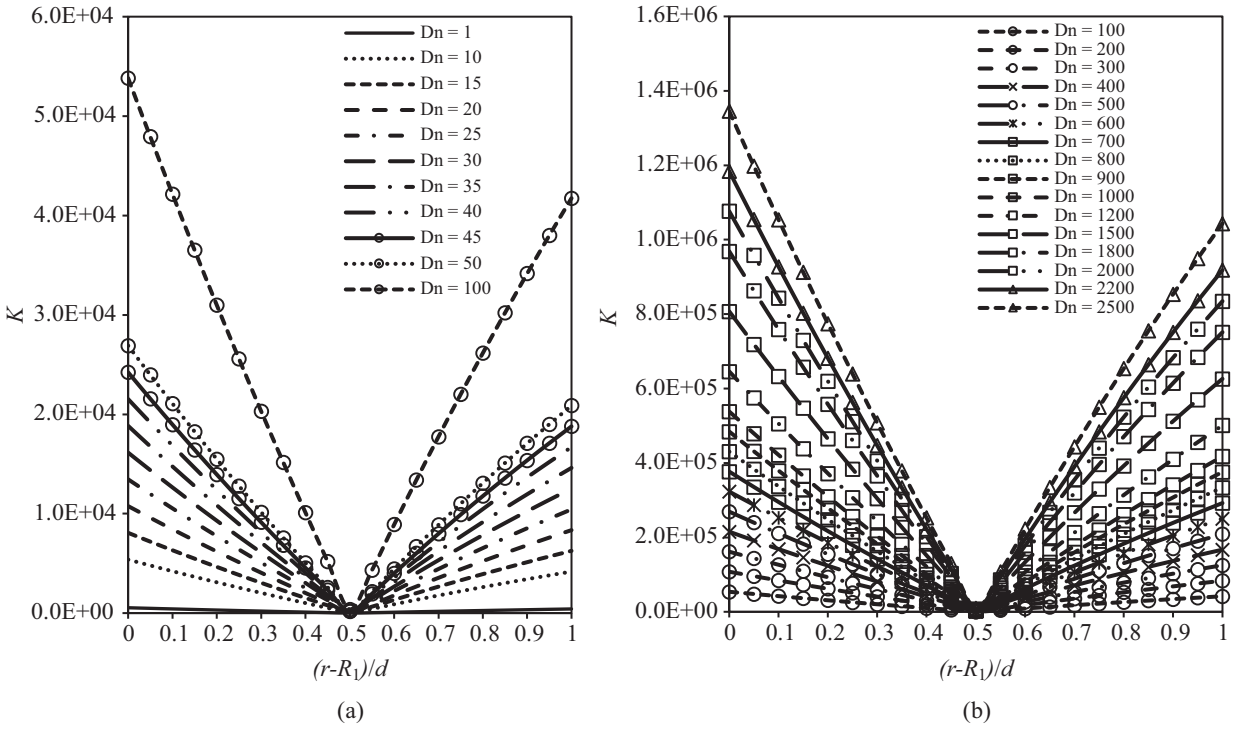


Fig. 7 Distribution of dimensionless parameter of energy gradient function K at different Dean numbers under $\delta = 0.1$ and T = 293.15 K; (a) Dn = 1 to Dn = 100; (b) Dn =100 to 2500.

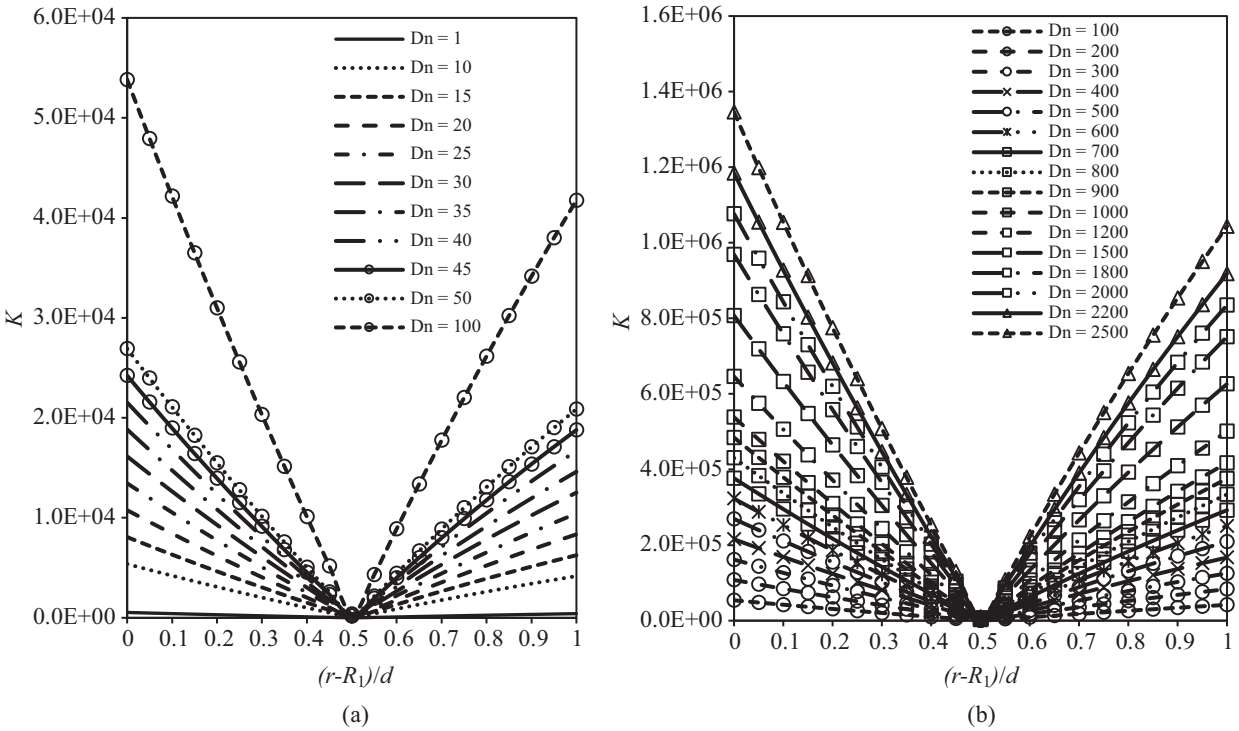


Fig. 8 Distribution of dimensionless parameter of energy gradient function K at different Dean numbers under $\delta = 0.1$ and T = 298.15 K; (a) Dn = 1 to Dn = 100; (b) Dn = 100 to 2500.

all three considered temperature. Moreover, the largest values of K are located respectively on the inner and outer walls of the parallel curved walls and the maximum of K is evident on the inner wall ($r - R_1/d = 0$). In addition, based on Figs. 7, 8 and 9, one can be concluded that, the value of K is decreased linearly with high slope from inner wall to the center of the gap ($r - R_1/d = 0.5$) and then it is increased linearly with lower slope from center

https://doi.org/10.1017/jmech.2017.112 Published online by Cambridge University Press

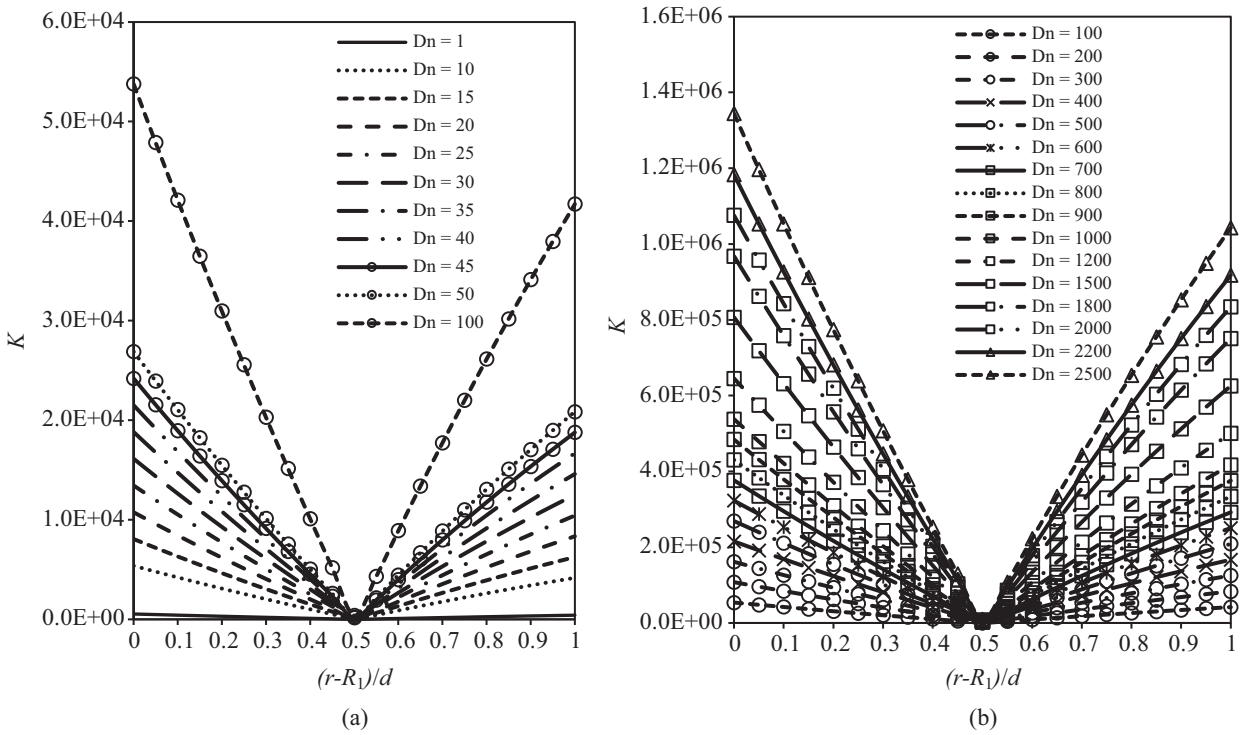


Fig. 9 Distribution of dimensionless parameter of energy gradient function K at different Dean numbers under $\delta = 0.1$ and T = 303.15 K; (a) Dn = 1 to Dn = 100; (b) Dn = 100 to 2500.

of the gap to the outer wall. Indeed, the minimum of K is occurred at the peak of the velocity profile (see Figs. 4, 5 and 6) which is in accordance with Dou and Ben study [34]. Therefore, the stability of the flow is dominated by the K_{max} at the inner wall and the onset of flow instability will be predicted in the proximity of inner wall in the tested conditions.

Comparing between Figs. 7, 8 and 9 show that the different temperatures have a negligible impression on the maximum of K value and its distribution under different Dean numbers. However, in section 4.2, we focus a detail study on the effects of temperatures on the velocity profile and energy gradient function K in Dean flow.

4.2 Effects of Temperature

As may be found in literature [2, 11, 16, 24], the critical Dean number for onset of instability is equal to 35.92. So, at this critical Dean number, we investigate the effects of different temperatures on the velocity profile and dimensionless energy gradient function K at small curvature $\delta = 0.1$ under different temperatures in Figs. 10 and 11, respectively. As may be seen in Fig. 10, at the fixed critical Dean number 35.92, as the temperature increases, the peak of velocity profile is decreased. In addition, corresponding to Fig. 11, we deduced that different temperatures have an insignificant effect on the K value and consequently on the fluid flow instability. Regarding to Fig. 11(b), irregular behavior and difference is detectable for K value under different temperatures at critical Dean number 35.92. The reason of this fact may be related to change of dynamic viscosity, kinematic viscosity and density of considered fluid (i.e. water) under different temperatures. Indeed, on one hand, as temperature increases, dynamic viscosity, kinematic viscosity and density of water will be decreased. On the other hands, for fixing the Dean number, azimuthal pressure gradient $\left(\partial p / \partial \theta\right)_0$ is increased when the temperature increases. Consequently, regarding to this reasons, irregular changes are obtained for K value by increase of fluid flow temperature.

It should also be noted that our considered viscous incompressible fluid (i.e. water) having temperature-dependent viscosity and density. Therefore, changing the temperature will vary the thermophysical properties of density and viscosity of considered incompressible fluid, however, the change of density is small [35-37]. For more details about the values of water density and viscosity under different temperature, we can refer to Ref. [38].

4.3 Effects of Curvature Ratio

One of the effective geometrical factors on hydrodynamic instability of Dean flow is curvature ratio. For study on the effects of different curvature ratios on the behavior of fluid flow, velocity profile and dimensionless energy gradient function K at T = 298.15 K and critical Dean number 35.92 are presented in Figs. 12 and 13, respectively. As may be seen in Figs. 12 and 13, due to great changes of velocity value and K under different curvature ratios, we presented these diagrams in the logarithmic scale. Moreover, to change of curvature ratio, we change the value of R_2 at the fixed $R_1 = 1$. Accord-

https://doi.org/10.1017/jmech.2017.112 Published online by Cambridge University Press

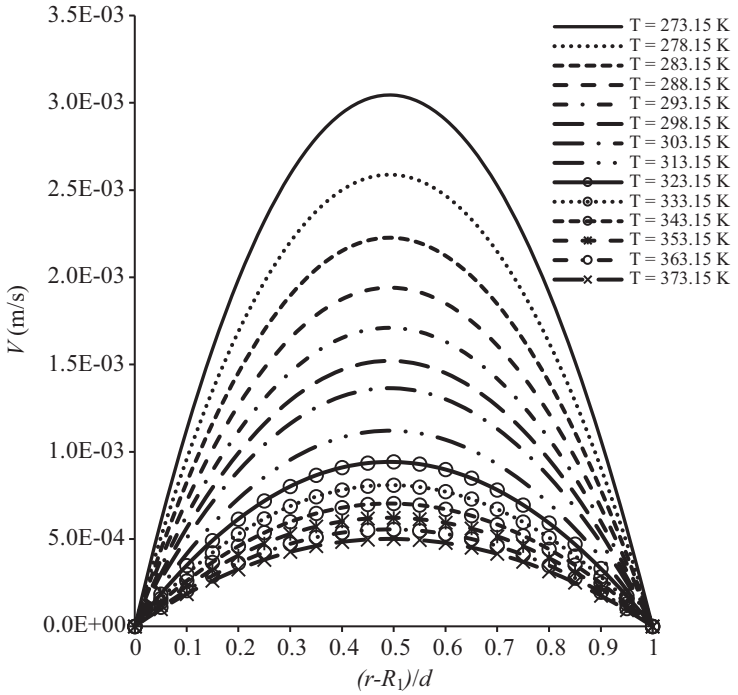
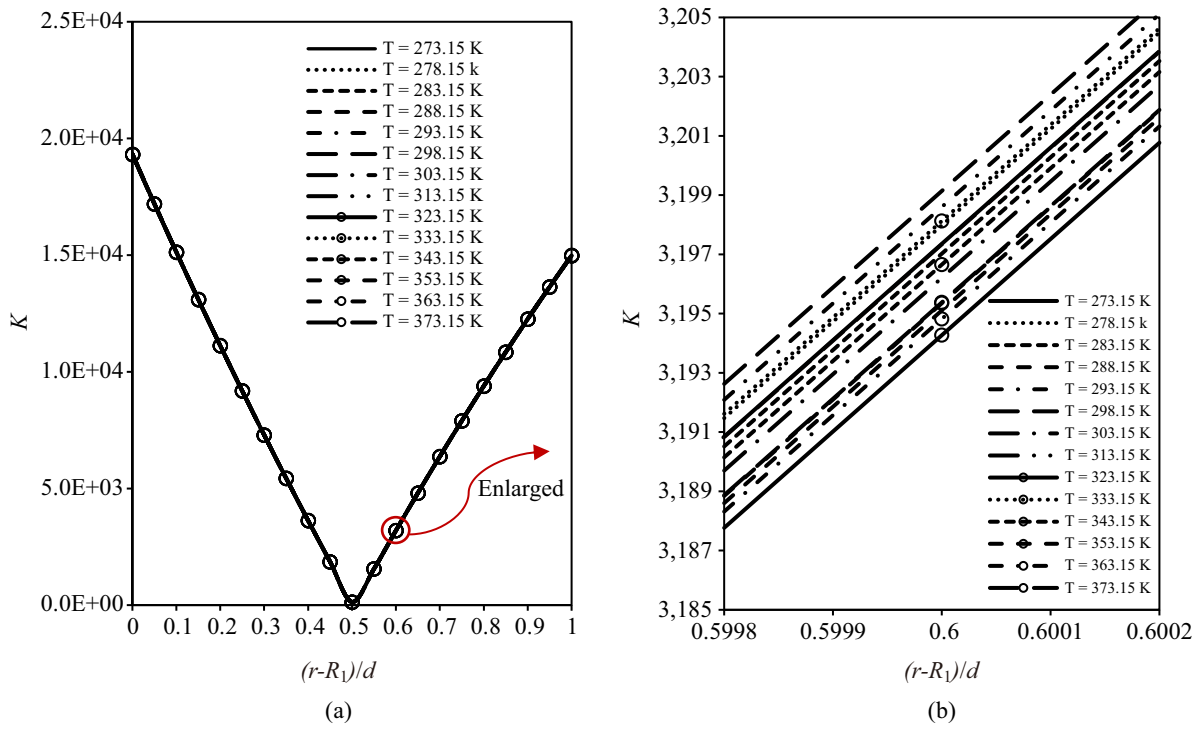


Fig. 10 Velocity profile at different temperature under δ = 0.1 and Dn = 35.92.



(a) (b)

Fig. 11 (a) Distribution of dimensionless parameter of energy gradient function K at different temperatures under δ = 0.1 and Dn = 35.92, (b) Enlarged diagram.

ing to Fig. 12, it is visible that, larger curvature ratio leads to lower value in velocity profile. As may be seen in Fig. 13, by decrease of curvature ratios, the K value is increased. As a result, with decrease of curvature ratio, the probability of onset of instability will be increased that is in accordance with Walowit *et al*. [16]. Indeed, by increase of curvature ratios at fixed Dean number, the energy gradient in cross-stream direction is significantly decreased compared to energy gradient in stream-wise direction (i.e. viscosity friction). In addition, at lower curvature ratios, maximum of K value is evident on both sides of inner and outer walls, where we expect that the

https://doi.org/10.1017/jmech.2017.112 Published online by Cambridge University Press

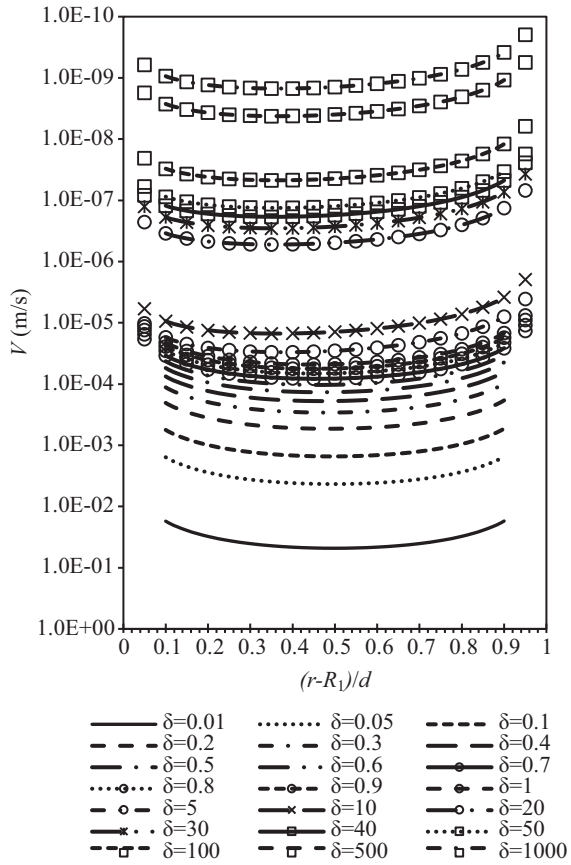


Fig. 12 Velocity profile at different curvature ratio under T = 298.15 K and Dn = 35.92.

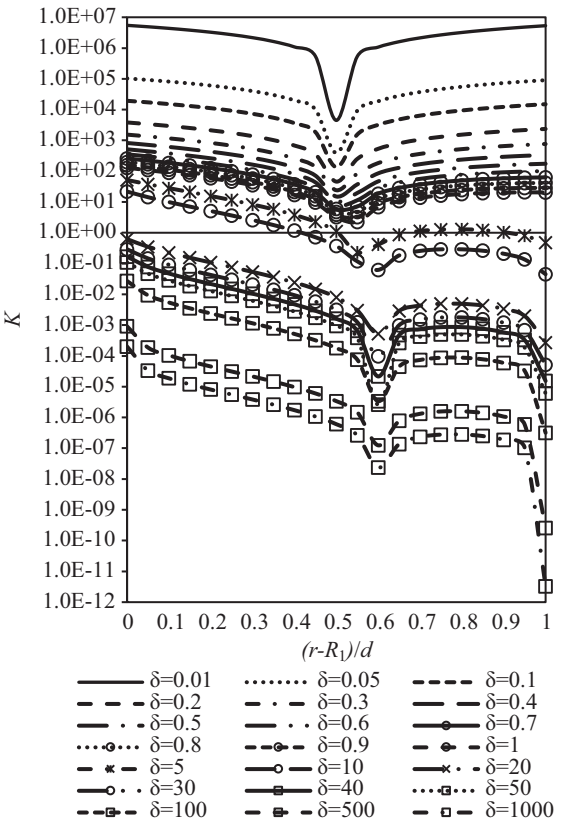


Fig. 13 Distribution of parameter of energy gradient function K at different curvature ratio under T = 298.15 K and Dn = 35.92.

instability will be originated from these local regions. However, at large curvature ratio, especially after $\delta > 5$, the maximum of K value is observable on the inner wall, and the value of K on the outer wall is insignificant. So, we expect that the onset of instability at large curvature ratio will be originated near the inner wall.

To comprehensively investigate on the critical condition for flow instability in Dean flow under different curvature ratios, the maximum value of energy gradient function K_{max} versus the Dean numbers at room temperature of T = 298.15 K is depicted in Fig. 14. According to Fig. 14, the maximum values of energy gradient function K_{max} are increased by decrease of curvature ratios. Moreover, at each curvature ratio, the K_{max} is linearly increased by increasing of Dean number under logarithmic scale.

By using energy gradient method, we calculate the critical energy gradient function K_c at the critical Dean numbers reported in literature (i.e. archival studies [2, 16 and 24]) as may be seen in Table 1. It's notable that, in the archival studies [2, 16 and 24] that reported the critical Dean numbers, the curvature ratio and inner radius R_1 aren't determined precisely and they have only referred to expression of "the very small curvature". Therefore, in Table 1, calculated critical energy gradient function K_c corresponds to archival critical Dean numbers are reported under four small curvatures of $\delta = 0.1$, $\delta = 0.01$, $\delta = 0.001$ and $\delta = 0.0001$, where we assumed $R_1 = 1$.

5. CONCLUSIONS

We investigated the hydrodynamic instability of Dean flow at comprehensive different Dean numbers ranging from 1 to 2500, different curvature ratios in range of 0.0001 to 1000 and temperatures ranging from 273.15 K to 373.15 K by using energy gradient method. We compared our normalized analytical velocity profile with existing archival data and acceptable agreement is obtained. Four main conclusions of the present study are deduced as follows:

(1) Under different temperatures, by increase of Dean number at fixed small curvature ratio, the value of K increases and it causes to destabilizing of Dean fluid flow.

(2) At critical Dean number, increase of the curvature ratio is resulted to reduce of the energy gradient function K in the whole flow field. Thus, it leads to the flow becomes more stable.

(3) Increase of the fluid flow temperatures leads to decrease of the peak of velocity profile, however, at given critical Dean number, we can't find any regular and significant effects of temperature on the energy gradient function K.

(4) We found that the values of K_{max} occur respectively on the inner and outer walls of the Dean flow geometry and therefore, the origin of instability in the entire flow field of a Dean flow is located on vicinity of these walls. Moreover, by increase of

https://doi.org/10.1017/jmech.2017.112 Published online by Cambridge University Press

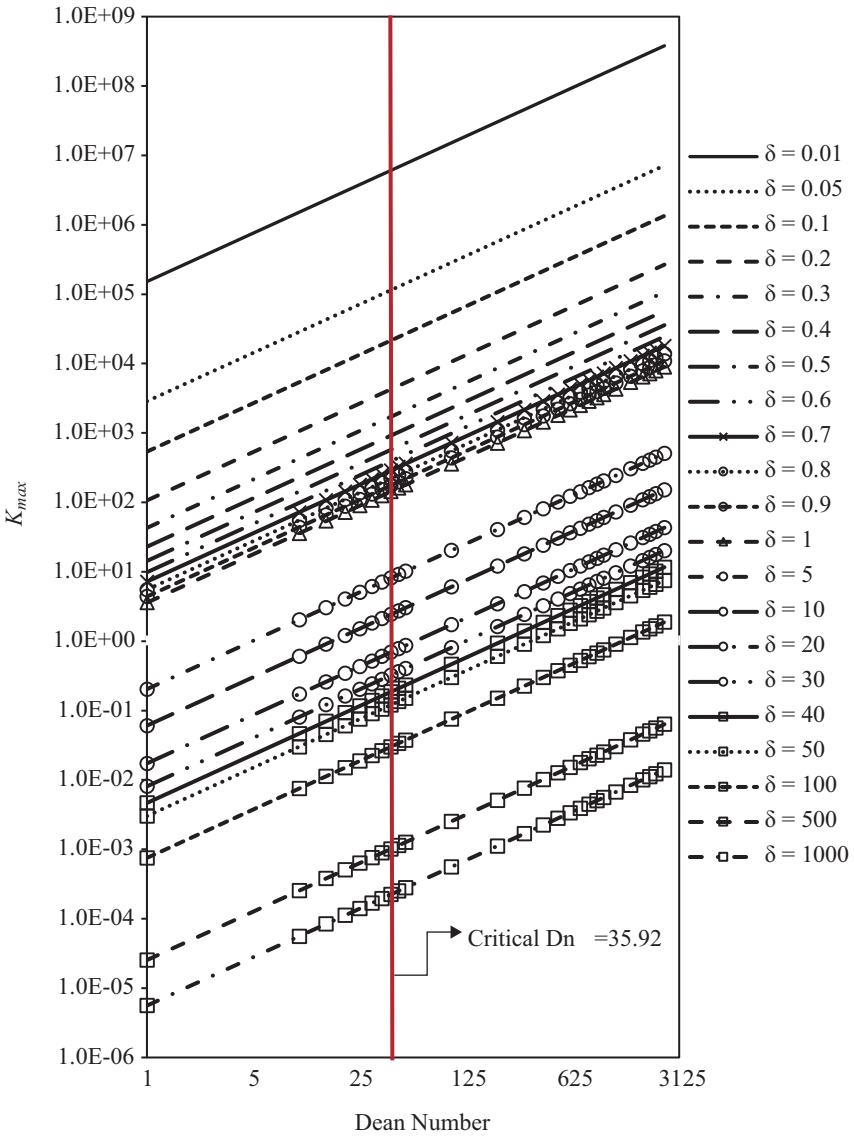


Fig. 14 Maximum of energy gradient function K_{max} vs Dean numbers at room temperature of T = 298.15 K under different curvature ratios.

Table 1 Critical energy gradient function K_c at four different assumed curvature ratios (δ) under critical Dean numbers extracted from archival data [2, 16 and 24] (at room temperature T = 298.15 K).

Dnc reported in archival studies		Calculated K_c at the present Study			
Ref.	Dn_c	δ = 0.1 & R_1/R_2 = 0.9090	δ = 0.01 & R_1/R_2 = 0.9900	δ = 0.001 & R_1/R_2 = 0.9990	δ = 0.0001 & R_1/R_2 = 0.9999
Dean [2]	35.95	19351.59	5466429	1708146703	539542811524.25
Walowit *et al.*[16]	35.90	19324.67	5458826	1705770977	538792404275.53
Deka and Paul [24]	35.922	19336.52	5462171	1706816296	539122583465.41

the curvature ratios, the probability of onset of instability near the inner walls will be increased.

Finally, it can be concluded that the energy gradient method is capable theory to investigate of flow field stability and the current research merits further study in future including study on the effects of different fluids types in Dean flow.

ACKNOWLEDGEMENTS

The authors would like to express their appreciation to Dr. Hua-Shu Dou from Zhejiang Sci-Tech University for his helpful comments.

https://doi.org/10.1017/jmech.2017.112 Published online by Cambridge University Press

REFERENCES

1. Drazin, P. G. and Reid, W. H., *Hydrodynamic Stability*, 2nd Edition, Cambridge University Press, Cambridge (2004).
2. Dean, W. R., "Fluid Motion in a Curved Channel," *Proceedings of the Royal Society of London, Series A*, **121**, pp. 402-420 (1928).
3. Joseph, B., Smith, E. P. and Adler, R. J., "Numerical Treatment of Laminar Flow in Helically Coiled Tubes of Square Cross Section: Part I. Stationary Helically Coiled Tubes," *AIChE Journal*, **21**, pp. 965-974 (1975).
4. Cheng, K. C., Lin, R. C. and Ou, J. W., "Fully Developed Laminar Flow in Curved Rectangular Channels," *Journal of Fluid Engineering*, **98**, pp. 41-48 (1976).
5. Ghia, K. N. and Sokhey, J. S., "Laminar Incompressible Viscous Flow in Curved Ducts of Regular Cross-Sections," *Journal of Fluid Engineering*, **99**, pp. 640-648 (1977).
6. Cheng, K. C. and Yuen, F. P., "Flow Visualization Experiments on Secondary Flow Patterns in an Isothermally Heated Curved Pipe," *Journal of Heat Transfer*, **109**, pp. 55-61 (1987).
7. Masliyah, J. H., "On Laminar Flow in Curved Semicircular Ducts," *Journal Fluid Mechanics*, **99**, pp. 469-479 (1980).
8. Dennis, S. C. R., "Dual Solutions for Steady Laminar Flow through a Curved Tube," *The Quarterly Journal of Mechanics and Applied Mathematics*, **35**, pp. 305-324 (1982).
9. Hille, P., Vehrenkamp, R. and Schulz-Dubois, E. O., "The Development and Structure of Primary and Secondary Flow in a Curved Square Duct," *Journal Fluid Mechanics,* **151**, pp. 219-241 (1985).
10. Li, Y., Wang, X., Yuan, S. and Tan, S. K., "Flow Development in Curved Rectangular Ducts with Continuously Varying Curvature," *Experimental Thermal and Fluid Science*, **75**, pp. 1-15 (2016).
11. Reid, W. H., "On the Stability of Viscous Flow in a Curved Channel," *Proceedings of the Royal Society of London, Series A*, **244**, pp. 186-198 (1958).
12. Reid, W. H. and Harris, D. L., "Some Further Results on the Bénard Problem," *Physics of Fluids*, **1**, pp. 102-110 (1958).
13. Bahl, S. K., "The Effect of Radial Temperature Gradient on the Stability of a Viscous Flow between Two Rotating Coaxial Cylinders," *Journal of Applied Mechanics*, **39**, pp. 593-595 (1972).
14. Chandrasekar, S., *Hydrodynamic and Hydromagnetic Stability*, Oxford University Press, London (1961).
15. Zhiming, L. and Yulu, L., "A Calculation Method for Fully Developed Flows in Curved Rectangular Tubes," *Applied Mathematics and Mechanics*, **18**, pp. 315-320 (1997).
16. Walowit, J., Tsao, S. and DiPrima, R. C., "Stability of Flow between Arbitrarily Spaced Concentric Cylindrical Surfaces Including the Effect of a Radial Temperature Gradient," *Journal of Applied Mechanics*, **31**, pp. 585-593 (1964).
17. Deka, R. K. and Takhar, H. S., "Hydrodynamic Stability of Viscous Flow between Curved Porous Channels with Radial Flow," *International Journal of Engineering Science*, **42**, pp. 953-966 (2004).
18. Orszag, S. A., "Accurate Solution of the Orr- Sommerfeld Stability Equation," *Journal Fluid Mechanics*, **50**, pp. 689-703 (1971).
19. Yamamoto, K., Yanase, S. and Jiang, R., "Stability of the Flow in a Helical Tube," *Fluid Dynamics Research*, **22**, pp. 153-170 (1998).
20. Mondal, R. N., Islam, M. Z., Islam, M. M. and Yanase, S., "Numerical Study of Unsteady Heat and Fluid Flow through a Curved Rectangular Duct of Small Aspect Ratio," *Thammasat International Journal of Science and Technology*, **20**, pp. 1-20 (2015).
21. Helal, M. N. A., Ghosh, B. P. and Mondal, R. N., "Numerical Simulation of Two-Dimensional Laminar Flow and Heat Transfer through a Rotating Curved Square Channel," *American Journal of Fluid Dynamics*, **6**, pp.1-10 (2016).
22. Yanase, S., Kaga, Y. and Daikai, R., "Laminar Flows through a Curved Rectangular Curved Duct over a Wide Range of Aspect Ratio," *Fluid Dynamics Research*, **31**, pp. 151-183 (2002).
23. Canuto, C., Hussaini, M. Y., Quarteroni, A. and Thomas, Jr. A., *Spectral Methods in Fluid Dynamics*, Springer-Verlag, Berlin (2012).
24. Deka, R. K. and Paul, A., "Stability of Taylor–Couette and Dean Flow: A Semi-Analytical Study," *Applied Mathematical Modeling*, **37**, pp. 1627-1637 (2013).
25. Dou, H. S., "Energy Gradient Theory of Hydrodynamic Instability," *The Third International Conference on Nonlinear Science*, Singapore (2004).
26. Dou, H. S., "Mechanism of Flow Instability and Transition to Turbulence," *International Journal of Non-Linear Mechanics*, **41**, pp. 512-517 (2006).
27. Mahapatra, T. R., Dholey, S. and Gupta, A. S., "Stability Of Hydromagnetic Dean Flow between Two Arbitrarily Spaced Concentric Circular Cylinders in The Presence of a Uniform Axial Magnetic Field," *Physics Letters A*, **373**, pp. 4338-4345 (2009).
28. Dou, H. S., "Three Important Theorems for Fluid Dynamics," *arXiv Preprint Physics/0610082* (2006).
29. Dou, H. S., Khoo, B .C. and Yeo, K. S., "Energy Loss Distribution in the Plane Couette Flow and the Taylor–Couette Flow between Concentric Rotating Cylinders," *International Journal of Thermal Sciences*, **46**, pp. 262-275 (2007).
30. Farahbakhsh, I., Nourazar, S. S., Ghassemi, H., Dou, H. S. and Nazari-Golshan, A., "On the Instability of

https://doi.org/10.1017/jmech.2017.112 Published online by Cambridge University Press

Plane Poiseuille Flow of Two Immiscible Fluids Using the Energy Gradient Theory," *Journal of Mechanics*, **30**, pp. 299-305 (2014).

31. Nowruzi, H., Nourazar, S. S. and Ghassemi, H., "On the Instability of Two Dimensional Backward-Facing Step Flow Using Energy Gradient Method," *Journal of Applied Fluid Mechanics*, **11**, pp. 241-256 (2018).
32. Topakoglu, H. C., "Steady Laminar Flows of an Incompressible Viscous Fluid in Curved Pipes," *Journal of Mathematics and Mechanics*, **16**, pp. 1321-1337 (1967).
33. Siggers, J. H. and Waters, S. L., "Steady Flows in Pipes with Finite Curvature," *Physics of Fluids*, **17**, 077102 (2005).
34. Dou, H. S. and Ben, A. Q., "Simulation and Instability Investigation of the Flow around a Cylinder between Two Parallel Walls," *Journal of Thermal Science*, **24**, pp. 140-148 (2015).
35. Hossain, M. A., Munir, M. S. and Rees, D. A. S., "Flow of Viscous Incompressible Fluid with Temperature Dependent Viscosity and Thermal Conductivity Past a Permeable Wedge with Uniform Surface Heat Flux," *International Journal of Thermal Sciences*, **39**, pp. 635-644 (2000).
36. Wang, C., Liu, S., Wu, J. and Li, Z., "Effects of Temperature-Dependent Viscosity on Fluid Flow and Heat Transfer in a Helical Rectangular Duct with a Finite Pitch," *Brazilian Journal of Chemical Engineering*, **31**, pp. 787-797 (2014).
37. Kafoussias, N. G. and Williams, E. W., "The Effect of Temperature-Dependent Viscosity on Free-Forced Convective Laminar Boundary Layer Flow Past a Vertical Isothermal Flat Plate," *Acta Mechanica*, **110**, pp. 123-137 (1995).
38. Speight, J. G., *Lange's Handbook of Chemistry*, 17th Edition, McGraw-Hill, New York (2005).

(Manuscript received October 2, 2017,
accepted for publication December 3, 2017.)

https://doi.org/10.1017/jmech.2017.112 Published online by Cambridge University Press